The Use of Continuous and Discrete Markers for Solving Hydrodynamic Problems with Movable Interface Boundaries

Nikolay G. Burago[1], Alexander D. Nikitin[2], and Ilia S. Nikitin[2(✉)]

[1] Ishlinsky Institute for Problems in Mechanics of the RAS, 101-1, Prosp. Vernadskogo Moscow, 119526 Moscow, Russian Federation
buragong@ya.ru

[2] Institute of Computer Aided Design, RAS, 19/18 2-Ya Brestskaya Ul, 123056 Moscow, Russian Federation
nikitin_alex@bk.ru, i_nikitin@list.ru

Abstract. Algorithms and results of continuous and discrete markers methods application to the problem of heavy viscous fluid flows calculations with free boundaries are described. The three-dimensional non-stationary Navier-Stokes equations and finite element method are used in variational formulation. An interface capturing method is implemented using fixed-grid with a continuous marker-function and (alternatively) discrete Lagrangian markers. The marker-functions have jumps at the interfaces and the interface boundary is detected as a level surface with intermediate value of marker-function. In numerical solutions, such way to detect interface boundary may result in the conservation laws violation even if conservative numerical methods are used. In order to prevent such effects in our algorithms the procedures of marker-function antidiffusion and conservation laws correction are introduced. In addition, in algorithms an immediate removal of possible monotonicity violations is used. Another implemented way to capture moving interfaces is based on the use of discrete Lagrangian markers. In addition to classic variant of the Marker And Cell (MAC) method, the algorithms of creation of new markers and removal of old markers at input and output boundaries are used. It allows us to consider the problems with open boundaries at long times. The improved interpolation at interface boundaries is described. The methods of continuous and discrete markers are used to simulate some set of incompressible viscous fluid flows with moving free boundaries and variable topology of solution region (joining and separation of parts of solution region). The solutions for following flows are presented: (1) falling water drop into water basin, (2) the flow of water from floor to floor through the hole, (3) the collapse of a water column and the oscillations of a fluid in a closed basin, (4) a fountain and a puddle from a vertical jet, and (5) fall of horizontal jets into the pool with water.

Keywords: Heavy viscous fluid · Moving interface boundaries
Free boundaries · Continuous markers · Discrete markers · Finite elements

I. B. Petrov et al. (Eds.): GCM50 2018, SIST 133, pp. 185–198, 2019.
https://doi.org/10.1007/978-3-030-06228-6_16

1 Introduction

History of research on flows with moving interface boundaries including free, contact, and phase transfer boundaries is highlighted in review [1]. Remind major facts concerning interface boundaries calculations in hydrodynamics. There are at least four categories of methods modeling flows with moving interface boundaries.

Methods of the first category for interface capture use two grids: the first grid is a fixed structured or unstructured grid in the area of possible multiphase fluid motion, and the second grid is the surface grid at the moving interface boundary. Methods of the second category capture the interface boundary as a level surface of continuous marker-function defined on fixed spatial grid covering the possible fluid motion area and having definite constant value for each phase. Methods of the third category trace the situation of phases by using Lagrangian (moving with material media) discrete markers so that each phase has its own set of markers. At last, methods of the fourth category are meshless. Such methods consider Lagrangian markers as material particles having mass, impulse, energy, vorticity, electric charge, and possibly other physical characteristics. Remark that history and implementation of another approach to modeling of processes with movable interfaces is considered in [2], where two movable Arbitrary Lagrange-Eulerian (ALE) adaptive overlapping meshes are used.

The rest of the chapter is organized as follows. Section 2 briefly reviews four categories of methods. A problem statement is given in Sect. 3. A numerical method is reported in Sect. 4. The features of the methods of continuous and discrete markers are discussed in Sects. 5 and 6, respectively. Section 7 gives the conclusions.

2 Related Work

Consider the main four categories of methods for modeling flows with moving interface boundaries in Sects. 2.1 and 2.4, respectively.

2.1 Methods of the First Category

Methods of the first category are the most accurate for interface boundary motion detection. In most studies, the first grid is fixed (unmovable) and Cartesian ijk-grid. Second grid is moving unstructured surface grid at the interface boundary represented by triangles in 3D geometry and segments in 2D case. The moving grid is defined by time dependent nodal coordinates and by the script of cell node numbers. This allows easy detection of normal vector and curvature for use in boundary conditions. Firstly, the moving grid of surface discrete markers was introduced in [3]. Further development of surface markers is highlighted in [4]. Significant improvement of the interface boundary calculation is achieved in [5] due to local grid refinement in fixed grid cells with surface markers.

During coalescence and separation of domains occupied by some phase the topology of interface boundary is changed. This makes the script of cell node numbers dependent on time. In 2D case, the implementation of such topology changes in calculations may be done. However, even in this case the grid algorithms become very

complex and inconvenient. In 3D case, the implementation of variable in time surface grid topology strikes with practically unsolvable difficulties. These difficulties exactly correspond to difficulties in calculations of flows with exact detection of multiple shocks using Rankine-Hugoniot conditions. More detailed analysis of surface marker and grid methods is presented in review [6].

2.2 Methods of the Second Category

A continuous Lagrangian marker is a function that takes the given values for each phase and defines the interface as the surface of an equal level of the marker function. The marker-function $C(\mathbf{x}, t)$ obeys the transport equation:

$$\frac{dC(\mathbf{x},t)}{dt} = 0 \quad \text{or} \quad \frac{\partial C(\mathbf{x},t)}{\partial t} + \mathbf{u}(\mathbf{x},t) \cdot \nabla C(\mathbf{x},t) = 0,$$

where $\mathbf{u}(\mathbf{x}, t)$ is a velocity of material medium. Gradient of the marker-function at the interface boundary points the direction of normal vector. Curvature of interface boundary is defined by second derivatives of marker function. The evolution of the marker-function is defined by a through calculation on grids covering the spatial region of motion of the media in question.

A typical representative of the second category is volume of fluid method [Volume of Fluid or Volume of Fraction (VOF)] [7]. In this method, the ratio of the fluid-filled part of the cell volume to its total cell volume plays the role of marker function. Parameters of the interface geometry are determined using the marker-function and a special algorithm. In the case of formation of multiple partially-filled cells, the determination of the interface in this method may become impossible.

In similar concentration or color methods of the marker-function takes given constant values for each phase and at the interface boundary has a jump. When integrating the equation for the marker function, it is necessary in this case: (1) to minimize the numerical diffusion of the marker function at the interfaces and (2) to ensure the monotonicity of the difference scheme (otherwise, the volume of the fluid, for pure numerical reasons, will fall into drops corresponding to false maxima and minima of the marker-function).

In the method of level set functions (see the reviews [8, 9]), the marker function determines the distance from a given point to the interface, which is positive for points in this phase and negative for points beyond its boundaries. Due to a smooth change in this function, when passing through the interface, the diffusion effect of the marker-function on the interface is insignificant but for long duration the values of the marker-function already lose their meaning as distances to the boundary and, therefore, from time to time the distances to the boundary are redefined during the calculation.

In all methods of continuous markers, there is a problem associated with violations of conservativeness due to errors in determining the interface boundaries as surfaces of an equal level of the marker function. For long duration, these violations lead to a loss of the physical meaning of the numerical solution, which is especially noticeable when conservation of mass is violated.

The boundary conditions at the immersed interfaces (free boundary, surface tension, phase transition conditions, etc.) are taken into account in the differential formulation by including in the equations integral terms with delta functions [10–12]. In the numerical implementation, the delta function involved in the equations is approximated by the ordinary capping function with the finite thickness assigned to the interface that makes possible to ensure stability and smoothness of the solution in the neighborhood of the boundary.

More details on history and methods of second category can be found in [1, 13–17].

2.3 Methods of the Third Category

The methods of the third category are similar to those of the first category. The region of possible medium motion is covered by an Euler fixed grid, and instead of second Lagrangian surface grid, the position of the phases is determined by the arrangement of Lagrangian discrete markers covering the region of space occupied by a medium of a certain phase and moving together with this medium. The first version of the MAC method was presented in [18, 19] and developed in [20, 21].

Each marker is characterized by coordinate values that indicate its position in space and the number that determines the type of phase, to which the marker belongs. The coordinates of the marker $\mathbf{x}(t)$ are determined by integrating the differential equation of Lagrangian trajectories $d\mathbf{x}/dt = \mathbf{u}(\mathbf{x}, t)$. In most MAC-method versions, discrete markers are not combined into meshes, so the implementation of complex boundary conditions using normals and curvatures is often not envisaged.

There are no fundamental difficulties in the determination of the curvature and the normals to the interface in the discrete markers methods. To determine the boundaries, the markers of a given phase on each time layer can be quickly combined into a grid of Dirichlet cells, then the boundary will be formed by those edges (2D) or faces (3D) that are not common for two Dirichlet cells. Another way to determine the interface is to assign a marker phase index to the nearest Eulerian mesh node. Then interface boundaries can be defined as isosurfaces passing through cells with a variable phase index function.

2.4 Methods of the Fourth Category

At the turn of the 1980s, a large category of meshless particle methods appeared. In these methods, the Lagrangian markers were transformed into material particles, namely, they are supplied with mass, momentum, energy, vorticity, electric charge, and other attributes of the material medium. The conservation laws (balance equations) in such methods are formulated using the Galerkin-Petrov method and the expansion of the solution with respect to finite basis functions that defined without the use of grids. The history and more detailed description of these methods can be found in reviews [1, 22, 23].

Also, here the category of mixed material particle-cell methods should be mentioned (see reviews [24, 25]).

In the presented here study, we use only the simplest versions of the continuous and discrete Lagrangian markers methods on fixed Eulerian grids. We describe useful and

very simple ways to realize these methods that ensure the necessary efficiency. Also, we present the results of these simplified methods application to typical problems of flows with free boundaries.

3 Problem Statement

Consider the motion of a heavy incompressible viscous fluid. The original equations have the form:

$$\rho(\partial_t \mathbf{u} + \mathbf{u} \cdot \nabla \mathbf{u}) = -\nabla p + \nabla \cdot \boldsymbol{\sigma}_v + \rho \mathbf{g}$$
$$\nabla \cdot \mathbf{u} = 0$$
$$\partial_t \rho + \mathbf{u} \cdot \nabla \rho = 0,$$

where the equation of motion, the incompressibility condition, and the transport equation for the density are written in traditional notations, the viscous stress tensor is determined by the Coulomb-Newton law $\boldsymbol{\sigma}_v = \mu(\nabla \mathbf{u} + (\nabla \mathbf{u})^T)$, the coefficient of dynamic viscosity μ assumed to be given.

The variational form of the equations is:

$$\int_V [\rho(\partial_t \mathbf{u} + \mathbf{u} \cdot \nabla \mathbf{u} - \mathbf{g}) \cdot \delta \mathbf{u} + (-p\mathbf{I} + \boldsymbol{\sigma}_v + \rho v_u \nabla \mathbf{u}) \cdot \nabla \delta \mathbf{u}] dV = \int_S \mathbf{n} \cdot (-p\mathbf{I} + \boldsymbol{\sigma}_v) \cdot \delta \mathbf{u} dS,$$

$$\int_V \left[(\partial_t \rho + \mathbf{u} \cdot \nabla \rho) \cdot \delta \rho + v_\rho \nabla \rho \cdot \nabla \delta \rho \right] dV = 0,$$

where the pressure is determined by the incompressibility condition using the penalty method $p = -\rho_0 c^2 \tau_0 \nabla \cdot \mathbf{u}$. The penalty for violating the incompressibility condition allows a small compressibility of the fluid, the coefficient $\rho_0 c^2 \tau_0$ plays the role of the penalty coefficient, constant c plays the role of the speed of sound (the speed of propagation of small perturbations), the constant factor τ_0 has the dimension of time. For small Mach numbers $M = |\mathbf{u}|/c \ll 1$, the fluid behaves as incompressible.

Additional diffusion terms with kinematic viscosity coefficients v_u and v_ρ in the equations are introduced, since such terms in the equations inevitably appear in the form of explicit or implicit artificial viscosity necessary to ensure the stability of numerical algorithms.

We assume that the fluid in the general case is inhomogeneous (it has different values of the density in the subdomains) and contains mobile interface boundaries in the domain V.

At the initial instant of time, the distribution of density and velocity is given by the initial conditions:

$$t = 0, \quad \mathbf{x} \in V : \rho = \rho_0(\mathbf{x}), \quad \mathbf{u} = \mathbf{u}_0(\mathbf{x}).$$

The conditions on the boundaries of the solution region, as well as at the interfaces, have the form of constraints on the boundary values of the unknown functions or the corresponding fluxes and are taken into account in the variational equations in well known manner using penalty or Lagrange multipliers.

4 Numerical Method

The basis of the numerical method is a two-layer central-difference scheme obtained by applying the simplest piecewise linear spatial finite-element approximation of variational equations. The convective terms of the equations are approximated by an explicit scheme and an explicit artificial viscosity is used to ensure the stability of the scheme. Artificial viscosity is adopted in the form:

$$\nu_u = |\mathbf{u}|h/2,$$

where h is the characteristic cell size (finite element size).

To improve the simulation of the boundary layers, the physical viscosity is reduced in accordance with the Samarskii method of exponential fitting in the simplest version:

$$\mu_u = \mu_{u0}^2/(\mu_{u0} + \rho\nu_u),$$

where the index "0" indicates the initial uncorrected values.

We note that the viscous (diffusion) and penalty terms of the equations are approximated implicitly. To find the solutions of the implicit scheme, a matrix-free iterative method of conjugate gradients is used, each iteration exactly reproduces the calculation of the time step of an explicit two-layer central-difference scheme. To find a solution, no more than $\sqrt{N}$ iterations are required (N is the number of unknowns). Due to a good initial approximation (solution on the previous time layer), the number of iterations actually falls to two or three, so that implicitness is not associated with appreciable additional costs of computing work.

The time step is limited by the stability condition (explicit scheme for convection):

$$\Delta t \leq \min_{k\in\Omega}\{h_k/|\mathbf{u}_k|\},$$

where Ω is a set of cell numbers k.

For used numerical method local conservativeness or the balance of fluxes between the nodal volumes is a consequence of the variational formulation and the fact that the derivative of the constant is equal to zero.

5 Features of the Method of Continuous Markers

In our case, the role of a continuous marker plays the density of incompressible fluids. There can be several fluids and each of them has its own density, in particular, the zero density corresponds to the empty space. The motion of fluids is determined from the

solution of the transfer equation. The interface is then defined as the surface of an equal level of the marker function.

Important components of solution algorithm are monotonization and correction of conservativeness procedures.

If non-monotonic algorithms are used to calculate the velocity and density (marker function!), the subdomain occupied by the fluid will very quickly become a set of disjointed droplets with boundaries defined by isolines (isosurfaces) of the continuous marker $\rho = 0.5$. It will happen due to false maxima and minima of the marker-function.

A characteristic sign of the nonmonotonicity of the method is the so-called "saw" on the graphs of the solution along the given line or on the isolines figure. The "saw" is present if the sign of the second derivative along some direction is changed at the ends of grid rib (the grid rib is a line connecting neighboring nodes). The directions of the rib and coordinate line are not required to coincide.

Second derivatives of function $w(\mathbf{x})$ in the case of piecewise linear approximation are calculated as solutions of the following variational equation:

$$\int_V (w_{xx} - \partial^2 w/\partial x^2)\delta w_{xx} dV = 0.$$

Integrating by parts one gets the following equation:

$$\int_V w_{xx}\delta w_{xx} dV + \int_V \partial w/\partial x \partial w_{xx}/\partial x dV = \int_S \partial w/\partial x \delta w_{xx} n_x dV,$$

where solution domain V has boundary S. We assume that the right part of the equation is equal to zero. It means that first or second derivative of function in question is zero at the boundary S. For the first integral in the left part of the equation the Gaussian quadrature with nodal integration points is used. It leads to explicit algorithm for second derivatives calculation. Second derivations along y and z coordinates are calculated in the same way.

We use the following very simple formula to correct monotonicity violations:

$$\rho_i^{n+1} = (\rho_{i*}^{n+1} + (\rho_{i*-1}^{n+1} + \rho_{i*+1}^{n+1})/2)/2,$$

where values in the right part with ± 1 in lower indices are calculated using interpolation along coordinate direction with violation of monotonicity. Such correction is not conservative but the conservativeness will be corrected further. Also it should be mentioned that the number of nodes with monotonicity violation is much less than total nodal number.

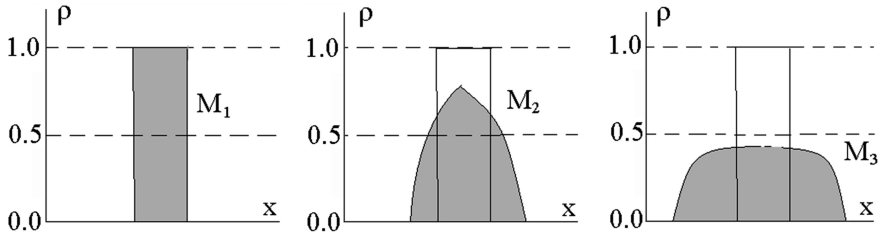

Fig. 1. Continuous marker method errors when determining the area filled with a fluid.

Thus, let for new time layer we have monotonous marker-function distribution. Consider three density distributions in the 1D solution domain shown in Fig. 1. The integral of the density over the solution domain gives the same mass value for all three distributions $(M_1 = M_2 = M_3)$. But if, according to the method of the continuous marker, we take a level line $\rho = 0.5$ as interface boundary, then we get for the incompressible fluid following strange results:

(a) In the state 2 fluid occupies a larger volume than in the state 1.
(b) In the state 3 fluid is disappeared.

This defect in the continuous marker method is a consequence of the diffusion of a continuous marker function, which undergoes a jump at the interfaces (in particular, at free boundaries).

To correct the defect, anti-diffusion of the marker function jumps of the marker function at the interfaces is used (its graphic representation is shown in Fig. 2).

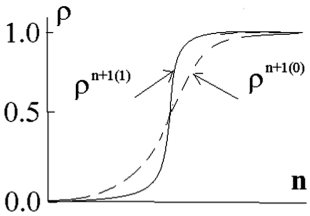

Fig. 2. Anti-diffusion of the continuous marker function at the interface.

Consider the algorithm of antidiffusion on a simple example of a free boundary. Let the density of the fluid be $\rho = 1.0$, while the value $\rho = 0.0$ corresponds to the empty space. Denote $\rho^{n+1(0)}$ the density value on the new time layer obtained by the monotonic conservative scheme described in Sect. 4. Let one of the possible antidiffusion algorithms has the form:

If $\rho^{n+1(0)} > 0.5$ and $\rho^{n+1(0)} > \rho^n$, then $\rho^{n+1(1)} = 1 - 2(1 - \rho^{n+1(0)})^2$,

If $\rho^{n+1(0)} \leq 0.5$ and $\rho^{n+1(0)} < \rho^n$, then $\rho^{n+1(1)} = 2(\rho^{n+1(0)})^2$.

The expected value of the mass in the domain of the solution by the algorithm from Sect. 4 is:

$$M^{n+1} = M^n - \int_S \rho^n \mathbf{u}^n \cdot \mathbf{n} dS,$$

where $M^n = \int_V \rho^n dV$. The value of mass obtained after application of anti-diffusion is equal to

$$M^{n+1(1)} = \int_V \rho^{n+1(1)} dV.$$

If $M^{n+1(1)} \neq M^{n+1}$ then the law of conservation of mass due to the application of antidiffusion is violated. To eliminate the error, the density is corrected by the formula:

$$\rho^{n+1} = \gamma \rho^{n+1(1)}, \quad \gamma = M^{n+1}/M^{n+1(1)}.$$

Thus, anti-diffusion prevents erosion of boundaries and does not violate mass conservatism. Of course, this is not the only possible way to prevent the diffusion of a continuous marker on the borders but it is quite workable and simple.

Below we present solutions of typical problems of the class considered obtained by the described method. Figure 3 shows the results of calculating the water drop falling into a water pool. Figure 4 shows the solution of the problem of heavy water flow from floor to floor through a hole. Figure 5 shows the collapse of a water column in a closed basin.

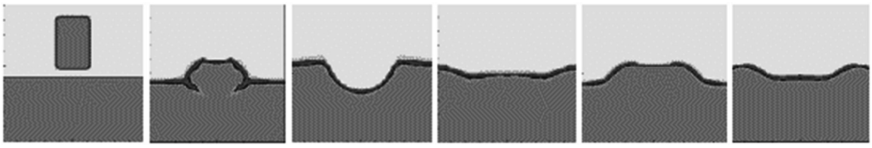

Fig. 3. Falling of drop into the pool. Heavy viscous incompressible fluid (Continuous marker function).

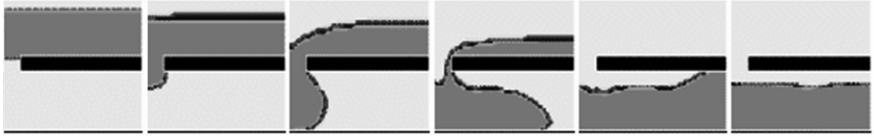

Fig. 4. Water flow from floor to floor through a hole. Heavy viscous incompressible fluid (Continuous marker function).

Note that in calculations without using the above described conservative antidiffusion algorithms for marker functions on the boundaries, the results are unsatisfactory because of the defects in mass conservation law mentioned above. In the problem of the collapsing of the water column to accelerate the attainment of the static state after several oscillations, the viscosity of the fluid was significantly increased; otherwise, the wave process lasted too long and required a large amount of computation.

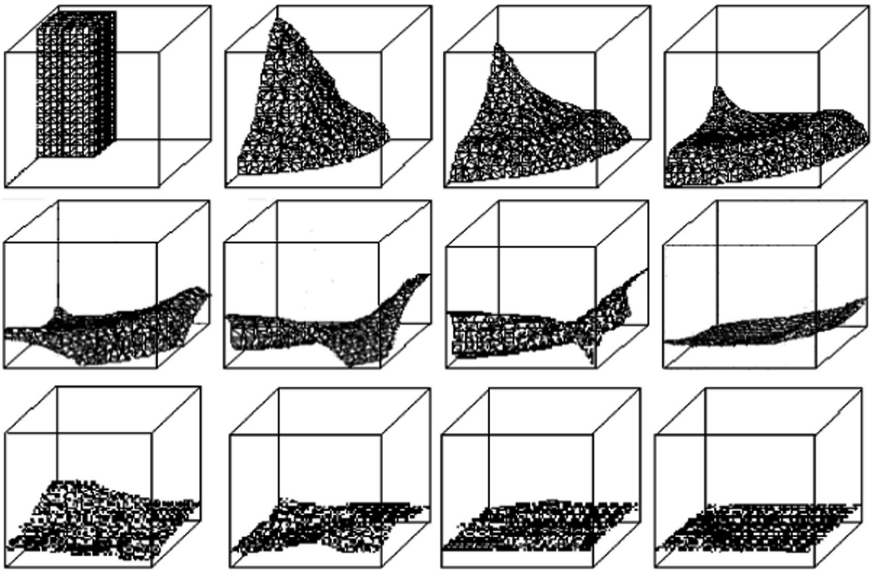

Fig. 5. Collapse of water column in closed basin. Heavy viscous incompressible fluid (Continuous marker function).

6 Features of the Discrete Marker Method

Instead of continuous marker functions used to trace moving areas occupied by a fluid, it is possible to use the discrete markers [19]. A discrete marker is a Lagrangian point (moving together with a continuous medium), the only property of which is the coordinates that indicate its position at each instant of time. The coordinates of the discrete marker with the number "i" are determined by integrating the equation of Lagrangian trajectories:

$$d\mathbf{x}_i/dt = \mathbf{u}_i.$$

Figure 6 shows fixed Cartesian grid and Lagrangian discrete markers that mark the area occupied by the fluid. It is assumed that nodal volume is filled by the fluid if in it at least one marker presents (left picture in Fig. 6). At the initial instant of time, the region of possible motion of the fluid is covered by a fringing Eulerian (fixed) grid consisting of nodes united in cells. In cells filled with fluid, discrete markers are introduced. It was experimentally established that to obtain satisfactory results in two-dimensional and three-dimensional cells, 3×3 and $3 \times 3 \times 3$ uniformly distributed discrete markers per cell should be used, respectively. Of course, more markers provides a better result but the markers require considerable computational effort, so here we give the advice on the minimum necessary number of them ($M = 3$, along the coordinate (rib) direction in the cell).

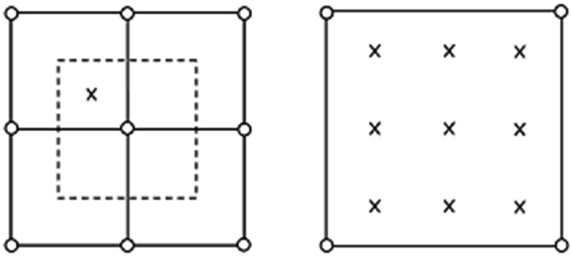

Fig. 6. Nodal volume in fixed Cartesian grid and Lagrangian discrete markers: **a** nodal volume (dashed line) with marker (cross), **b** initial distribution of markers in 2D cell with fluid ($M \times M$, $M = 3$).

In addition to the classical discrete marker method (see for instance [20]), here the algorithm provides the creation of new discrete markers at the input boundaries and the removal of discrete markers at the output boundaries. The main features of discrete marker method considered here are formulated below:

- 3D cell contains $M \times M \times M$ markers.
- 2D boundary cell contains $M \times M$ markers.
- Into cell at input boundary the $M \times M$ new markers are introduced if no markers present in boundary cell part of depth h/M (h is the size of cell in normal direction to the boundary).
- Markers leaving the solution area are removed from computer memory.
- Usual number of markers along coordinate (rib) is $M = 3 \div 4$.

In addition it should be mentioned that there are still the following computational problems present:

- Leakage of markers in the zones of strong topology changes (separation of drops in gravity field).
- Huge amount of calculations when increasing the number of markers.

Consider in detail the problem of flow parameters interpolation at interfaces. Let N be the number of nodes in the cell, and N^* is the number of nodes in the cell with markers in the nodal volumes. If $0 < N^* < N$, then the volume cell contains the interface (free boundary, for example). Then, in such cell (number k) we should use the interpolation procedure of the form:

$$[f]_k = \frac{1}{N^*} \sum_{i \in \Omega_k^*} f_i$$

instead of the usual:

$$[f]_k = \frac{1}{N} \sum_{i \in \Omega_k} f_i,$$

where Ω_k^* is a set of node numbers in the cell k with markers in nodal volumes. This prevents the unnatural effect of "shaggy head" in jets (see Fig. 7).

Fig. 7. The unnatural effect of "shaggy head" in jets (right picture).

Figures 8 and 9 give examples of calculating the fall of a horizontal jet into a pool with a fluid: without applying the interpolation procedure for the flow parameters at the interfaces (the "shaggy head" effect, Fig. 8) and using this procedure to eliminate an impermissible defect (Fig. 9).

Fig. 8. The unnatural effect of "shaggy head" when the jet falls into the pool.

Fig. 9. The jet falls into the pool. Effect of "shaggy head" is eliminated.

Figure 10 shows the results of calculating the problem of a fountain and a puddle from a vertical jet using the discrete marker method with the creation of new discrete markers at input boundaries and the removal of discrete markers at output boundaries (left and right boundaries are opened).

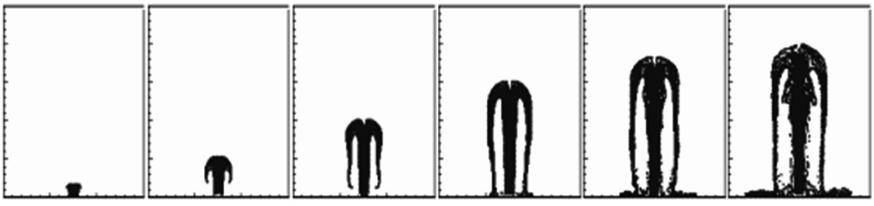

Fig. 10. A fountain and a puddle from a vertical jet.

Note that when the vertical jet reaches maximum height $H = u_{z0}^2/(2g)$ (here u_{z0} is a vertical velocity of jet at the input boundary, g is a gravity acceleration), it becomes unstable, looses symmetry and oscillates like a stream behind a bluff body at high Reynolds numbers.

7 Conclusions

The experience of using the methods of continuous and discrete markers for calculating the flows of a heavy viscous fluid with interface boundaries is presented. In the continuous marker method, complementary algorithms for monotonization and conservative boundary antidiffusion are proposed, algorithms for creating and destroying markers at input and output boundaries are introduced into the discrete marker method, interpolation of the solution near moving boundaries is improved. Solutions of a number of typical three-dimensional non-stationary problems on flows of a heavy viscous fluid with free boundaries are presented.

References

1. Burago, N.G., Kukudzhanov, V.N.: Review of contact algorithms. Mech. Solids **1**, 45–87 (2005)
2. Burago, N.G., Nikitin, I.S., Yakushev, V.L.: Hybrid numerical method for unsteady problems of continuum mechanics using arbitrary moving adaptive overlap grids. Comput. Math. Math. Phys. **56**(6), 1065–1074 (2016)
3. Noh, V.F.: Combined Eulerian-Lagrangian method for unsteady 2D problems. 3rd edn., Fundamental Methods in Hydrodynamics. Academic Press. New-York and London (1964)
4. Unverdi, S., Tryggvason, G.: A front-tracking method for viscous, incompressible, multi-fluid flows. J. Comput. Phys. **100**(1), 25–37 (1992)
5. Chen, S., Johnson, D.B., Raad, P.E., Fadda, D.: The surface marker and micro cell method. Int. J. Numer. Meth. Fluids **25**(7), 749–778 (1997)
6. Tryggvason, G., Bunner, B., Esmaeeli, A., Juric, D., Al-Rawahi, N., Tauber, W., Han, J., Nas, S., Jan, Y.-J.: A front tracking method for the computations of multiphase flow. J. Comput. Phys. **169**(2), 708–759 (2001)
7. Hirt, C.W., Nichols, B.D.: Volume of fluid (VOF) method for the dynamics of free boundaries. J. Comput. Phys. **39**(1), 201–225 (1981)
8. Osher, S., Fedkiw, R.P.: Level set methods: an overview and some recent results. J. Comput. Phys. **169**(2), 463–502 (2001)
9. Tan, Z., Lim, K.M., Khoo, B.C.: A level set-based immersed interface method for solving incompressible viscous flows with the prescribed velocity at the boundary. Int. J. Numer. Meth. Fluids **62**(3), 267–290 (2010)
10. Samarskii, A.A., Moiseenko, B.D.: Economical shock-capturing scheme for multi-dimensional Stefan problems. Comput. Math. Math. Phys. **5**(5), 816–827 (1965)
11. Peskin, C.S.: Numerical analysis of blood flow in the heart. J. Comput. Phys. **25**(2), 220–252 (1977)
12. Li, Z., Lai, M.-C.: The immersed interface method for the Navier-Stokes equations with singular forces. J. Comput. Phys. **171**(2), 822–842 (2001)

13. Shin, S., Juric, D.: Modeling three-dimensional multiphase flow using a level contour reconstruction method for front tracking without connectivity. J. Comput. Phys. **180**(2), 427–470 (2002)
14. Souli, M., Benson, D.J. (eds.) Arbitrary Lagrangian Eulerian and Fluid-Structure Interaction Numerical Simulation. London-Hoboken: ISTE Ltd. and Wiley (2010)
15. Ii, S., Sugiyama, K., Takeuchi, S., Takagi, S., Matsumoto, Y., Xiao, F.: An interface capturing method with a continuous function: The THINC method with multi-dimensional reconstruction. J. Comput. Phys. **231**(5), 2328–2358 (2012)
16. Hu, W.-F., Lai, M.-C., Young, Y.-N.: A hybrid immersed boundary and immersed interface method for electrohydrodynamic simulations. J. Comput. Phys. **282**, 47–61 (2015)
17. Patel, J.K., Natarajan, G.: Diffuse interface immersed boundary method for multi-fluid flows with arbitrarily moving rigid bodies. J. Comput. Phys. **360**, 202–228 (2018)
18. Harlow, F.H., Welch, J.E.: Numerical calculation of time-dependent viscous incompressible flow of fluid with free surface. Phys. Fluids **8**(12), 2182–2189 (1965)
19. Welch, J.E. Harlow, F.H., Shannon, J.P., Daly, B.J.: The MAC method. Los Alamos Scientific Laboratory Report, LA-3425 (1965)
20. Nickols, B.: Further development of the marker-in-cell method for incompressible fluid flow. In: Belotserkowskii O.M. (ed.) Numerical Methods in Fluid Mechanics, pp. 165–173. Mir. Moscow (1973) (in Russian)
21. Tome, M.F., McKee, S.: GENSMAC: A computational marker and cell method for free surface flows in general domains. J. Comput. Phys. **110**(1), 171–186 (1994)
22. Monaghan, J.J.: Smoothed particle hydrodynamics. Annu. Rev. Astron. Astrophys. **30**, 543–574 (1992)
23. Medin, S.A., Parshikov, A.N.: Development of smoothed particle hydrodynamics method and its application in the hydrodynamics of condensed matter. High Temp. **48**(6), 926–933 (2010)
24. Morgenthal, G., Walther J.: H. An immersed interface method for the Vortex-In-Cell algorithm. Comput. Struct. **85**(11–14), 712–726 (2007)
25. Palha, A., Manickathan, L., Carlos, S.F., Gerard, V.B.: A hybrid Eulerian-Lagrangian flow solver. arXiv:1505.03368 [math.NA], pp. 1–27 (2015)